4062 *Chem. Mater.* **2009,** *21,* 4062–4070
DOI:10.1021/cm9015222

CHEMISTRY OF MATERIALS
Article

Solution-Processable Novel Near-Infrared Electrochromic Aromatic Polyamides Based on Electroactive Tetraphenyl-*p*-Phenylenediamine Moieties

Hung-Ju Yen and Guey-Sheng Liou*

Functional Polymeric Materials Laboratory, Institute of Polymer Science and Engineering, National Taiwan University, 1 Roosevelt Road, Fourth Sec., Taipei 10617, Taiwan

Received June 3, 2009. Revised Manuscript Received July 19, 2009

A series of solution-processable near-infrared (NIR) electrochromic aromatic polyamides with *N*,*N*,*N*′,*N*′-tetraphenyl-*p*-phenylenediamine (TPPA) units in the backbone were prepared from the phosphorylation polyamidation reactions of a newly synthesized diamine monomer, *N*,*N*′-bis(4-aminophenyl)-*N*,*N*′-di(4-methoxylphenyl)-1,4-phenylenediamine, with various aromatic dicarboxylic acids. These polymers were readily soluble in many organic solvents and showed useful levels of thermal stability associated with high glass-transition temperatures (236−246 °C) and high char yields (higher than 58% at 800 °C in nitrogen). The polymer films showed reversible electrochemical oxidation with high contrast ratio both in the visible range and NIR region, which also exhibited high coloration efficiency (CE), low switching time, and the highest stability for long-term electrochromic operation to date. At the first oxidation stage, the polyamide **Ib** thin film revealed high coloration efficiency in visible (CE = 388 cm^2/C) and NIR (CE = 330 cm^2/C) region with reversible electroactive stability (over 10000 times within 0.4% loss relative to its initial injected charge). As the dication form of second oxidation stage, the polymer film still exhibited excellent electrochromic/electroactive stability (more than 3000 cyclic switches) with higher CE of 464 cm^2/C.

Introduction

Electrochromic materials exhibit a reversible optical change in absorption or transmittance upon electrochemically oxidized or reduced, such as transition-metal oxides, inorganic coordination complexes, organic molecules, and conjugated polymers.[1] Traditionally, investigation of electrochromic materials has been directed toward optical changes in the visible region (e.g., 400−800 nm), proved especially useful of variable reflectance mirrors, tunable windows, and electrochromic displays. Increasingly, attention of the optical changes has been focused extending from the near-infrared (NIR; e.g., 800−2000 nm) through the microwave regions of the spectrum,[2] which could be exploitable for environmental control (heat gain or loss) in buildings. Recently, NIR electrochromic materials such as transition metal oxides (WO3), quinone-containing organic materials, and organic metal complex (ruthenium dendrimer) have been investigated.[3] For organic materials, in addition to conjugated polymers,[4] *N*,*N*,*N*′,*N*′-tetraphenyl-*p*-phenylenediamine-containing molecule is a interesting anodic electrochromic system for NIR applications because of its particular intramolecular electron transfer in the oxidized states.

Intramolecular electron transfer (ET) processes were studied extensively in the mixed-valence (MV) systems,[5] and usually employed one-dimensional MV compounds contain two or more redox states. According to Robin and Day,[6] the *N*,*N*,*N*′,*N*′-tetraphenyl-*p*-phenylenediamine (TPPA) cation radical has been reported as a symmetrical delocalized class III structure with a strong electronic coupling (the electron is delocalized over the two redox centers), leading an intervalence charge transfer (IV-CT) absorption band in the NIR region.[7]

*Corresponding author. E-mail: gsliou@ntu.edu.tw.

(1) (a) Monk, P. M. S.; Mortimer, R. J.; Rosseinsky, D. R. *Electrochromism: Fundamentals and Applications*; VCH: Weinheim, Germany, 1995. (b) Mortimer, R. J. *Chem. Soc. Rev.* **1997**, *26*, 147. (c) Rosseinsky, D. R.; Mortimer, R. J. *Adv. Mater.* **2001**, *13*, 783. (d) Somani, P. R.; Radhakrishnan, S. *Mater. Chem. Phys.* **2003**, *77*, 117. (e) Liu, S.; Kurth, D. G.; Mohwald, H.; Volkmer, D. *Adv. Mater.* **2002**, *14*, 225. (f) Zhang, T.; Liu, S.; Kurth, D. G.; Faul, C. F. J. *Adv. Funct. Mater.* **2009**, *19*, 642. (g) Maier, A.; Rabindranath, A. R.; Tieke, B. *Adv. Mater.* **2009**, *21*, 959. (h) Motiei, L.; Lahav, M.; Freeman, D.; van der Boom, M. E. *J. Am. Chem. Soc.* **2009**, *131*, 3468.
(2) (a) Rose, T. L.; D'Antonio, S.; Jillson, M. H.; Kon, A. B.; Suresh, R.; Wang, F. *Synth. Met.* **1997**, *85*, 1439. (b) Franke, E. B.; Trimble, C. L.; Hale, J. S.; Schubert, M.; Woollam, J. A. *J. Appl. Phys.* **2000**, *88*, 5777. (c) Topart, P.; Hourquebie, P. *Thin Solid Films* **1999**, *352*, 243.
(3) (a) Vickers, S. J.; Ward, M. D. *Electrochem. Commun.* **2005**, *7*, 389. (b) Schwab, P. F. H.; Diegoli, S.; Biancardo, M.; Bignozzi, C. A. *Inorg. Chem.* **2003**, *42*, 6613. (c) Wang, S.; Todd, E. K.; Birau, M.; Zhang, J.; Wan, X.; Wang, Z. Y. *Chem. Mater.* **2005**, *17*, 6388–6394. (d) Qiao, W.; Zheng, J.; Wang, Y.; Zheng, Y.; Song, N.; Wan, X.; Wang, Z. Y. *Org. Lett.* **2008**, *10*, 641. (e) Qi, Y.; Wang, Z. Y. *Macromolecules* **2003**, *36*, 3146.
(4) (a) Sankaran, B.; Reynolds, J. R. *Macromolecules* **1997**, *30*, 2582. (b) Sonmez, G.; Meng, H.; Zhang, Q.; Wudl, F. *Adv. Funct. Mater.* **2003**, *13*, 726. (c) Sonmez, G.; Meng, H.; Wudl, F. *Chem. Mater.* **2004**, *16*, 574. (d) Dyer, A. L.; Grenier, C. R. G.; Reynolds, J. R. *Adv. Funct. Mater.* **2007**, *17*, 1480. (e) Li, M.; Patra, A.; Sheynin, Y.; Bendikov, M. *Adv. Mater.* **2009**, *21*, 1707.
(5) (a) Creutz, C.; Taube, H. *J. Am. Chem. Soc.* **1973**, *95*, 1086. (b) Lambert, C.; Noll, G. *J. Am. Chem. Soc.* **1999**, *121*, 8434.
(6) Robin, M.; Day, P. *Adv. Inorg. Radiochem.* **1967**, *10*, 247.

 Published on Web 08/07/2009

To be useful for electrochromic applications, some key issues such as long-term stability, rapid redox switching, high coloration efficiency (CE), and high optical transmittance change ($\Delta\%T$) during operation played important roles and are required to be achieved. Reynolds' group studied poly(3,4-ethylenedioxythiophene) (PEDOT) films and found that their electroactivity retained only 62% after 16 000 switching cycles with a contrast ratio less than 65%.[4a] The EDOT derivatives reported by Wudl's group exhibited a high CE and high stability after 5000 switching cycles, though it has a contrast ratio of only 57%.[4b,c] In our ongoing effort to develop electrochromic polymeric materials, we have synthesized and investigated a series of triphenylamine (TPA) containing high-performance polymers,[8] which showed good electrochromic reversibility in the visible region. In addition, we also prepared the analogous polymers bearing pendent variety moieties, and showed observable contrast ratio.[9] However, the NIR optical transmittance change and electrochromic stability of the anodically electrochromic materials in our previous studies provides still too low to allow for NIR electrochromic applications. Therefore, our strategy was to synthesize the highly stable NIR electroactive TPPA-based materials with the incorporation of electron-donating substituents at the para-position of phenyl groups, thus could greatly prevent the coupling reactions by affording stable cationic radicals and lowering the oxidation potentials.[10] The electroactive polymers with excellent thermal stability and high molecular weights could be obtained readily by using conventional polycondensation methods. Because of the incorporation of packing-disruptive TPPA units into the polymer backbone, most of the polymers exhibited good solubility in polar organic solvents, thus transparent and flexible polymer thin films could be prepared easily by solution casting and spin-coating techniques. This is beneficial for their fabrication of large-area, thin-film electrochromic devices.

In this contribution, we therefore synthesized the diamine monomer, *N*,*N*′-bis(4-aminophenyl)-*N*,*N*′-di(4-methoxylphenyl)-1,4-phenylenediamine [(OMe_2)TPPA-diamine; **2**], and its derived aromatic polyamides containing electroactive TPPA units with para-substituted methoxy groups. Polyamides as thermally stable microelectronic materials have attracted great interest. Incorporation of TPPA units into polyamides not only preserves some of the favorable properties such as high thermal stability, glass transition temperature, and the solubility for enhancing the film-forming ability but also provides the electroactive center to obtained polyamides facilitating both processing and application. Furthermore, the incorporation of electron-donating methoxy substituents is expected to reduce the oxidation potential associated with increased electrochemical and electrochromic stability of the result polyamides. We anticipated that the prepared electrochromic polyamides should be stable for multiple electrochromic switchings, improving optical response times, and enhancing CE with high optical density in NIR region. For a comparative study, some properties of the present polyamides will be compared with those of structurally related one based on *N*,*N*′-bis(4-aminophenyl)-*N*,*N*′-diphenyl-1,4-phenylenediamine [TPPA-diamine; **2**′] that has been reported previously.[11]

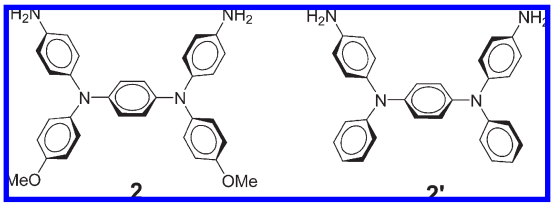

Results and Discussion

Monomer Synthesis. The new (OMe_2)TPPA-diamine monomer **2** was synthesized by hydrazine Pd/C-catalyzed reduction of the dinitro compound **1** resulting from the potassium carbonate-mediated aromatic nucleophilic substitution reaction of *N*,*N*′-di(4-nitrophenyl)-1,4-phenylenediamine with 4-iodoanisole, and 1,4-diiodobenzene with 4-methoxy-4′-nitrodiphenylamine, respectively (Scheme 1). Elemental analysis, FT-IR, and NMR spectroscopic techniques were used to identify structures of the intermediate dinitro compound **1** and the targeted diamine monomer **2**. The FT-IR spectra of these two synthesized compounds are illustrated in Figure S1 in the Supporting Information. The nitro groups of compound **1** exhibited two characteristic bands at around 1584 and 1308 cm^{-1} because of NO_2 asymmetric and symmetric stretching. After reduction to diamine monomer **2**, the characteristic absorption bands of the nitro group disappeared and the primary amino group showed the typical absorption pair at 3444 and 3359 cm^{-1} (N−H stretching). ^1H and ^{13}C NMR spectra of the dinitro

(7) Szeghalmi, A. V.; Erdmann, M.; Engel, V.; Schmitt, M.; Amthor, S.; Kriegisch, V.; Noll, G.; Stahl, R.; Lambert, C.; Leusser, D.; Stalke, D.; Zabel, M.; Popp, J. *J. Am. Chem. Soc.* **2004**, *126*, 7834.
(8) (a) Cheng, S. H.; Hsiao, S. H.; Su, T. X.; Liou, G. S. *Macromolecules* **2005**, *38*, 307. (b) Liou, G. S.; Hsiao, S. H.; Su, T. X. *J. Mater. Chem.* **2005**, *15*, 1812. (c) Liou, G. S.; Yang, Y. L.; Su, Y. L. O. *J. Polym. Sci., Part A: Polym. Chem.* **2006**, *44*, 2587. (d) Liou, G. S.; Hsiao, S. H.; Chen, H. W. *J. Mater. Chem.* **2006**, *16*, 1831. (e) Liou, G. S.; Hsiao, S. H.; Huang, N. K; Yang, Y. L. *Macromolecules* **2006**, *39*, 5337. (f) Liou, G. S.; Chen, H. W.; Yen, H. J. *J. Polym. Sci., Part A: Polym. Chem.* **2006**, *44*, 4108. (g) Liou, G. S.; Chen, H. W.; Yen, H. J. *Macromol. Chem. Phys.* **2006**, *207*, 1589. (h) Liou, G. S.; Chang, C. W.; Huang, H. M.; Hsiao, S. H. *J. Polym. Sci., Part A: Polym. Chem.* **2007**, *45*, 2004. (i) Liou, G. S.; Yen, H. J.; Chiang, M. C. *J. Polym. Sci., Part A: Polym. Chem.* **2009**No. DOI: 10.1002/pola.23587.
(9) (a) Liou, G. S.; Hsiao, S. H.; Chen, W. C.; Yen, H. J. *Macromolecules* **2006**, *39*, 6036. (b) Liou, G. S.; Yen, H. J. *J. Polym. Sci., Part A: Polym. Chem.* **2006**, *44*, 6094. (c) Yen, H. J.; Liou, G. S. *J. Polym. Sci., Part A: Polym. Chem.* **2009**, *47*, 1584.
(10) (a) Chang, C. W.; Liou, G. S.; Hsiao, S. H. *J. Mater. Chem.* **2007**, *17*, 1007. (b) Liou, G. S.; Chang, C. W. *Macromolecules* **2008**, *41*, 1667. (c) Hsiao, S. H.; Liou, G. S.; Kung, Y. C.; Yen, H. J. *Macromolecules* **2008**, *41*, 2800. (d) Chang, C. W.; Chung, C. H.; Liou, G. S. *Macromolecules* **2008**, *41*, 8441. (e) Chang, C. W.; Liou, G. S. *J. Mater. Chem.* **2008**, *18*, 5638. (f) Chang, C. W.; Yen, H. J.; Huang, K. Y.; Yeh, J. M.; Liou, G. S. *J. Polym. Sci., Part A: Polym. Chem.* **2008**, *46*, 7937.
(11) (a) Liou, G. S.; Hsiao, S. H.; Ishida, M.; Kakimoto, M.; Imai, Y. *J. Polym. Sci., Part A: Polym. Chem.* **2002**, *40*, 2810. (b) Liou, G. S.; Hsiao, S. H.; Fang, Y. K. *Eur. Polym. J.* **2006**, *42*, 1533.

Scheme 1. Synthetic Route to $(OMe)_2$TPPA-Diamine Monomer 2

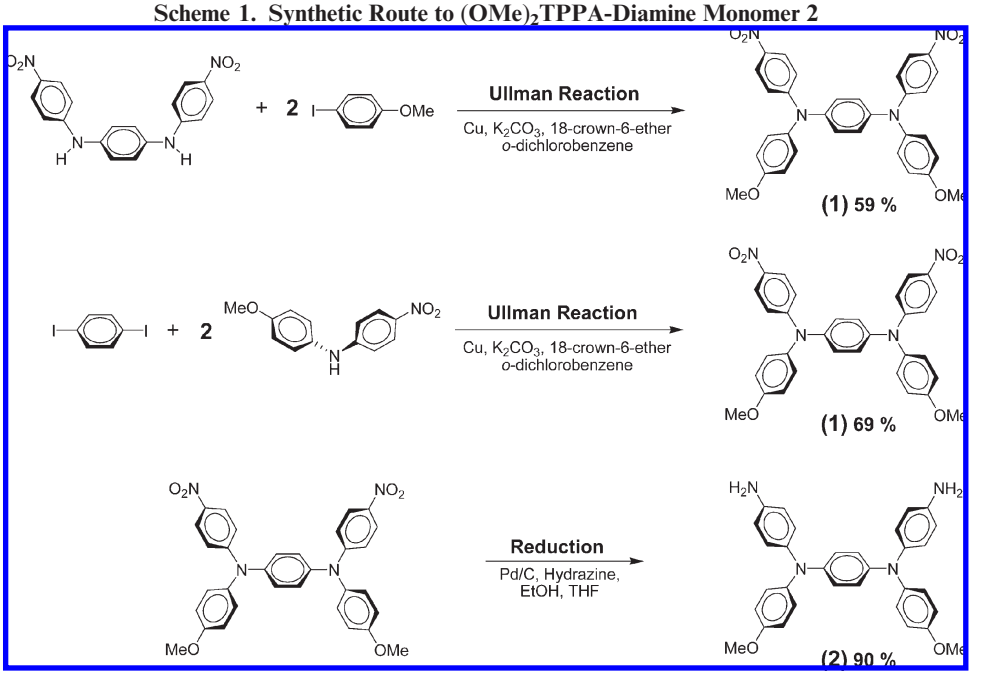

Scheme 2. Synthesis of Aromatic Polyamides Ia−Ic; Photograph Shows Appearance of the Flexible Films (thickness = 20−35μm)

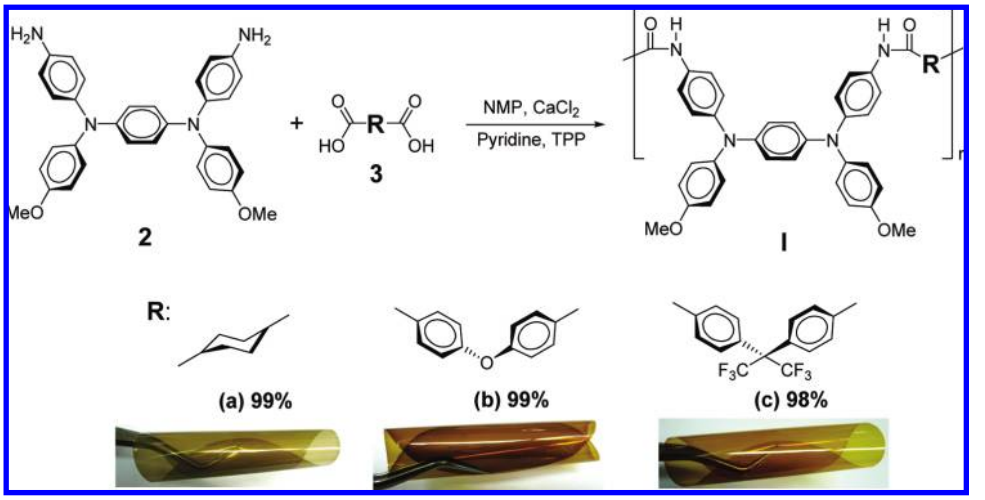

compound **1** and diamine monomer **2** are illustrated in Figure S2 and agree well with the proposed molecular structures.

Polymer Synthesis. According to the phosphorylation technique described by Yamazaki,[12] a series of novel polyamides **Ia−Ic** with main-chain (OMe_2)TPPA units were synthesized from the diamine monomer **2** with three aromatic dicarboxylic acids **3a−3c** (Scheme 2). The polymerization was carried out via solution polycondensation using triphenyl phosphite and pyridine as condensing agents. All polymerization reactions proceeded homogenously and gave high molecular weights. The obtained polyamides had inherent viscosities in the range of 0.48−0.73 dL/g with weight-average molecular weights (M_w) and polydispersity (PDI) of 49 000−237 800 Da and 1.45−1.94, respectively, relative to polystyrene standards (see Table S1 in the Supporting Information). All the high-molecular-weight polymers could afford transparent and tough films via solution casting. The structures of the polyamides were confirmed by IR spectroscopy. As shown in Figure S3 of the Supporting Information, a typical IR spectrum for polyamide **Ib** exhibited characteristic absorption bands of the amide group at around 3311 cm^{-1} (N−H stretch) and 1650 cm^{-1} (amide carbonyl). A structurally related polyamide **I'b** derived from TPPA-diamine **2'** is used for comparison studies. The synthesis and characterization of polymer **I'b** has been described previously.[11]

Solubility and Film Property. The solubility properties of polymers **Ia−c** were investigated qualitatively, and the results are also listed in Table S2 of the Supporting Information. Most of the polyamides were readily soluble in polar aprotic organic solvents such as *N*-methyl-2-pyrrolidinone (NMP), *N*,*N*-dimethylacetamide (DMAc),

(12) Yamazaki, N.; Matsumoto, M.; Higashi, F. *J. Polym. Sci., Polym. Chem. Ed.* **1975**, *13*, 1373.

N,*N*-dimethylformamide (DMF), dimethyl sulfoxide (DMSO), and *m*-cresol. Thus, the excellent solubility makes these polymers as potential candidates for practical applications by spin-coating or inkjet-printing processes to afford high performance thin films for optoelectronic devices. As mentioned earlier, the polyamides **Ia**−**Ic** could be solution cast into flexible, transparent, and tough films. As shown in Scheme 2, the cast films are transparent gray (for **Ia**) and light yellowish green (for **Ib** and **Ic**) in color. Their high solubility and amorphous properties can be attributed to the incorporation of bulky, three-dimensional (OMe_2)TPPA moiety along the polymer backbone, which results in a high steric hindrance for close packing, and thus reduces their crystallization tendency.

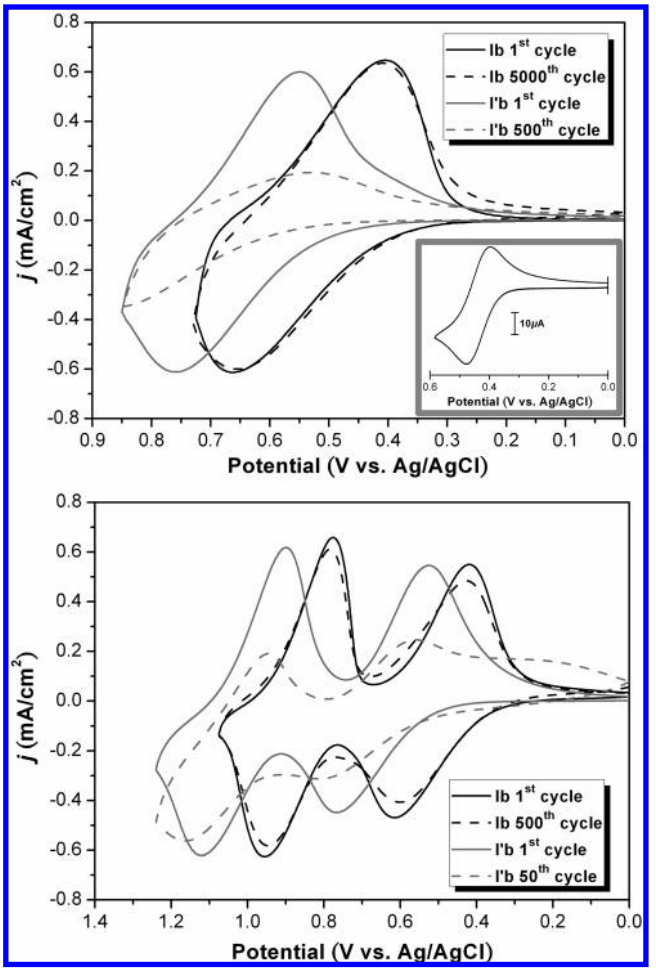

Figure 1. Cyclic voltammetric diagrams of polyamide **Ib** and **Ib** films on an ITO-coated glass substrate over cyclic scans and ferrocene (inset) in 0.1 M TBAP/CH_3CN at a scan rate of 50 mV/s.

Thermal Properties. The thermal properties of polyamides were examined by TGA and DSC, and the thermal behavior data are summarized in Table S2. Typical TGA curves of representative polyamides **Ib** and **I′b** in both air and nitrogen atmospheres are shown in Figure S4 of the Supporting Information. All the prepared polyamides exhibited good thermal stability with insignificant weight loss up to 450 °C under nitrogen or air atmosphere even with the introduction of methoxy groups. The 10% weight loss temperatures of these polymers in nitrogen and air were recorded in the range of 480−535 and 460−520 °C, respectively. The carbonized residue (char yield) of these polymers in a nitrogen atmosphere was more than 58% at 800 °C. The high char yields of these polymers can be ascribed to their high aromatic content. The glass-transition temperatures (T_g) of polyamides **Ia**−**Ic** could be easily measured in the DSC thermograms; they were observed in the range of 236−246 °C (as shown in Figure S5 of the Supporting Information), depending upon the stiffness of the polymer chain. The lowest T_g value of **Ib** in this series polymers can be explained in terms of the flexible ether linkage in its diacid component. All the polymers indicated no clear melting endotherms up to the decomposition temperatures on the DSC thermograms, which supports the amorphous nature of these polyamides. In Table S3 of the Supporting Information, polyamides **Ib** revealed a slightly lower T_g as compared to their respective analogs **I′b**. This result implies that the para-substitution of the methoxy group in the **I** series polyamides leads to an increase in steric hindrance for close chain packing, as well as an enhanced fractional free volume between polymer chains.

Electrochemical Properties. The electrochemical properties of the polyamides were investigated by cyclic voltammetry (CV) conducted for the cast film on an indium−tin oxide (ITO)-coated glass slide as working electrode in anhydrous acetonitrile (CH_3CN), using 0.1 M of tetrabutylammonium perchlorate (TBAP) as a supporting electrolyte under a nitrogen atmosphere. The typical CV for polyamides **Ib** (with 4,4′-dimethoxy-substituted) and **I′b** (without 4,4'-dimethoxy-substituted) are shown in Figure 1 for comparison; we observe two reversible oxidation redox steps at the half-wave potential ($E_{1/2}$) of 0.54 V (E_{onset} = 0.42) and 0.91 V for polyamide **Ib**, and 0.66 (E_{onset} = 0.55) and 1.02 V for polyamide **I′b**, respectively.

Table 1. Redox Potentials and Energy Levels of Polyamides

	thin films (nm)		oxidation potential (V)[a]					
			$E_{1/2}$		E_{onset}			
polymer	λ_{max}	λ_{onset}	first	second		E_g (eV)[b]	HOMO (eV)[c]	LUMO (eV)
Ia	312	399	0.50	0.88	0.40	3.11	4.84	1.73
Ib	342	411	0.54	0.90	0.42	3.02	4.86	1.84
Ic	308	415	0.55	0.91	0.44	2.99	4.88	1.89
I'b	341	402	0.66	1.02	0.55	3.08	4.99	1.91

[a] From cyclic votammograms versus Ag/AgCl in CH_3CN. $E_{1/2}$: Average potential of the redox couple peaks. [b] The data were calculated from polymer films by the equation: $E_g = 1240/\lambda_{onset}$ (energy gap between HOMO and LUMO). [c] The HOMO energy levels were calculated from cyclic voltammetry and were referenced to ferrocene (4.8 eV; onset = 0.36 V).

The lower oxidation potential of polyamide **Ib** compared to its analog **I'b** was resulted from the para-position substituted methoxy group on TPPA groups. During the electrochemical oxidation of the polyamide thin films, the color of the film changed from colorless to green and then to deep blue. Because of the high electrochemistry stability and good adhesion between the polyamide thin film and ITO substrate, polyamide **Ib** exhibited reversible CV behavior by continuous 5000 cyclic and 500 cyclic scans in the first and second oxidation stages, respectively. On the contrary, the corresponding polyamide **I′b** without the para-methoxy substituted on TPPA units gradually lost redox reversibility after several CV scans. This result also confirms that para-substitution of the methoxy group on the TPPA unit effectively increases stability for both the cation radical and dication quinonediimine species. The other polyamides showed similar CV curves to that of **Ib**. The redox potentials of the polyamides as well as their respective highest occupied molecular orbital (HOMO) and lowest unoccupied molecular orbital (LUMO) (versus vacuum) are shown in Table 1. The HOMO level or called ionization potentials (versus vacuum) of polyamides **Ia**−**Ic** are estimated from the onset of their oxidation in CV experiments as 4.84−4.88 eV (on the basis that ferrocene/ferrocenium is 4.8 eV below the vacuum level with $E_{onset} = 0.36$ V).

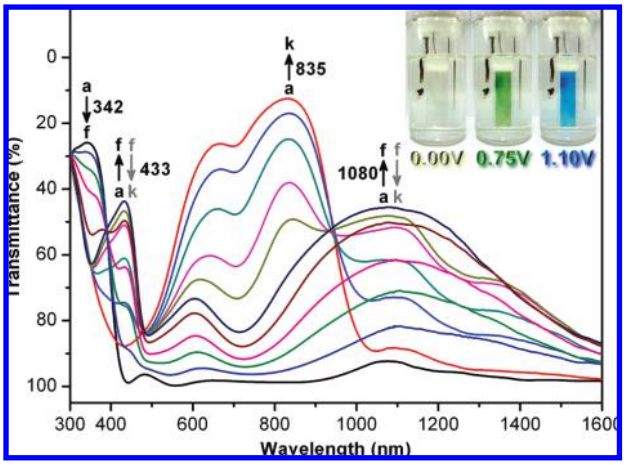

Figure 2. Electrochromic behavior of polyamide **Ib** thin film (~65 nm in thickness) on the ITO-coated glass substrate in 0.1 M TBAP/CH_3CN at applied potentials of (a) 0, (b) 0.40, (c) 0.50, (d) 0.60, (e) 0.70, (f) 0.75, (g) 0.80, (h) 0.85, (i) 0.93, (j) 1.00, (k) 1.10 (V vs Ag/AgCl). $\mathbf{Ib}^{+\cdot}$, black solid arrow; $\mathbf{Ib}^{2+}$, gray solid arrow.

Spectroelectrochemistry. Spectroelectrochemical experiments were used to evaluate the optical properties of the electrochromic films. For the investigations, the polyamide film was cast on an ITO-coated glass slide, and a homemade electrochemical cell was built from a commercial ultraviolet (UV)-visible cuvette. The cell was placed in the optical path of the sample light beam in a UV−vis−NIR spectrophotometer, which allowed us to acquire electronic absorption spectra under potential control in a 0.1 M TBAP/MeCN solution. The result of polyamide **Ib** film is presented in Figure 2 as a series of UV−vis−NIR absorbance curves correlated to electrode potentials. Figure 3 shows the three-dimensional % transmittance-wavelength-applied potential correlations of this sample. In the neutral form (0 V), the film exhibited strong absorption at around 342 nm, characteristic for

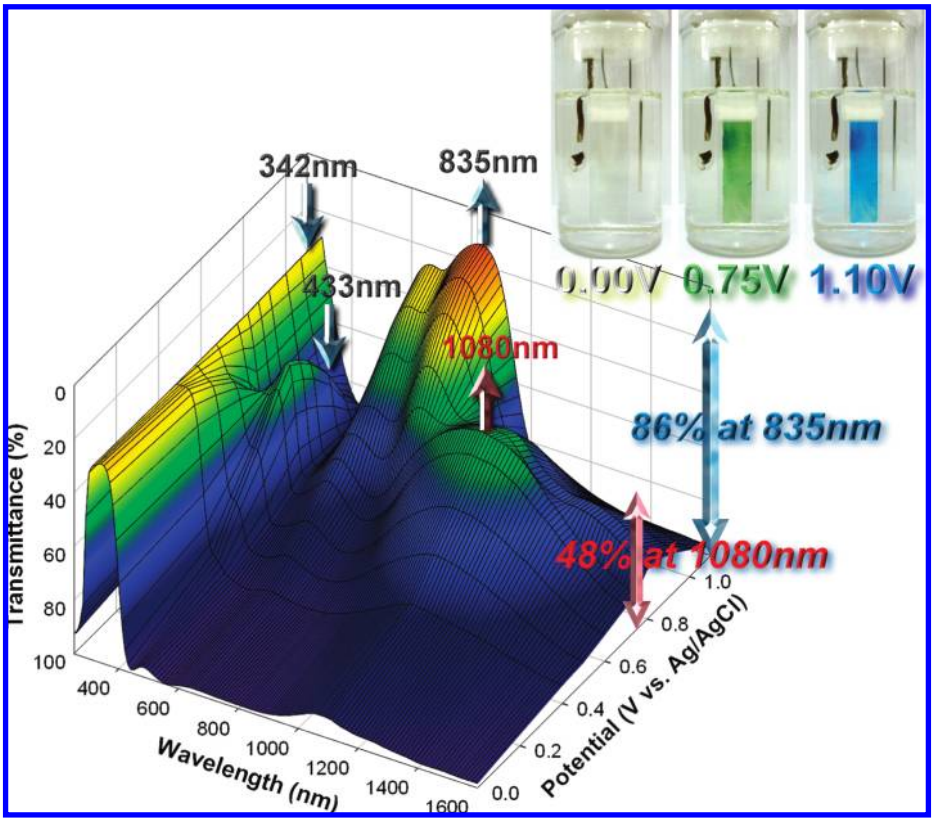

Figure 3. 3D spectroelectrochemical behavior of the **Ib** thin film on the ITO-coated glass substrate in 0.1 M TBAP/CH_3CN from 0 to 1.10 V (vs Ag/AgCl).

triarylamine, but it was almost transparent in the visible region. Upon oxidation (increasing applied voltage from 0 to 0.70 V), the intensity of the absorption peak at 342 nm gradually decreased, whereas a new peak at 433 nm and a broadband having its maximum absorption wavelength at 1080 nm in the NIR region gradually increased in intensity. We attribute the spectral change in visible range to the formation of a stable monocation radical of the TPA center in TPPA moiety. Furthermore, the broad absorption in NIR region was the characteristic result due to IV-CT excitation associated with ET from active neutral nitrogen atom to the cation radical nitrogen center of TPPA moiety, which was consistent with the phenomenon classified by Robin and Day.[6] As the more anodic potential to 1.10 V, the absorption bands of the cation radical decreased gradually with a new broadband centered at around 835 nm. The disappearance of NIR absorption band can be attributable to the further oxidation of monocation radical species to the formation of dication in the TPPA segments. The observed UV−vis−NIR absorption changes in the polyamide **Ib** film at various potentials are fully reversible and are associated with strong color changes. The other polyamides showed similar spectral change to that of **Ib**. From the inset shown in Figure 2, the polyamide **Ib** film switches from a transmissive neutral state (colorless; Y: 85; x, 0.313; y, 0.331) to a highly absorbing semioxidized state (green; Y: 40; x, 0.291; y, 0.442) and a fully oxidized state (deep blue; Y; 15; x, 0.178; y, 0.183). The film colorations are distributed homogeneously across the polymer film and survive for more than thousands of redox cycles. The polymer **Ib** shows good contrast both in the visible and NIR regions with an extremely high optical transmittance change ($\Delta\%T$) of 54% at 433 nm and 48% at 1080 nm for green coloring at the first oxidation stage, and 86% at 835 nm for blue coloring at the second oxidation stage, respectively. Because of the apparent high electrochromic contrast, optical switching studies were investigated more deeply to manifest the outstanding electrochromic characteristics of these obtained novel anodically electrochromic materials.

Electrochromic Switching Studies. For electrochromic switching studies, polymer films were cast on ITO-coated glass slides in the same manner as described above, and chronoamperometric and absorbance measurements were performed. Although the films were switched, the absorbance at the given wavelength was monitored as a function of time with UV−vis−NIR spectroscopy. Switching data for the representative cast film of polyamide **Ib** were shown in Figures 4 and 5. The switching time was calculated at 90% of the full switch because it is difficult to perceive any further color change with naked eye beyond this point. As depicted in Figure 4a, polyamide **Ib** thin film revealed switching time of 2.04 s at 0.70 V for coloring process at 433 nm and 1.21 s for bleaching. When the potential was set at 1.10 V, thin film **Ib** required 2.24 s for coloration at 835 nm and 1.47 s for bleaching (Figure 4b). The polyamides switched rapidly between the highly transmissive neutral state and the colored oxidized

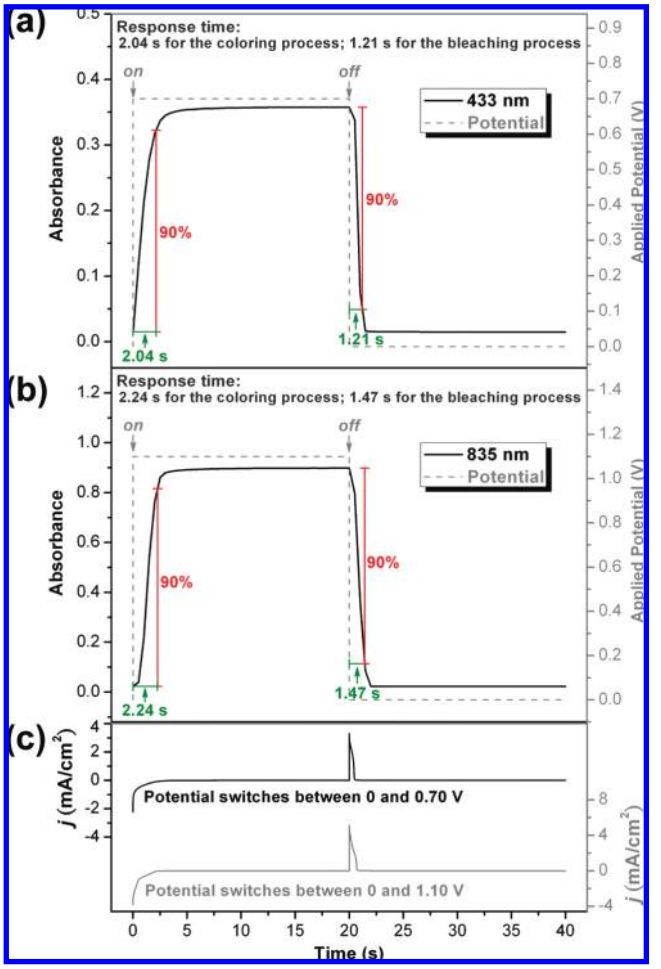

Figure 4. Calculation of optical switching time at (a) 433 nm, (b) 835 nm at the applied potential, and (c) current−time curves of polyamide **Ib** thin film (~65 nm in thickness) on the ITO-coated glass substrate (coated area: 1.1 cm × 0.5 cm) in 0.1 M TBAP/CH_3CN.

state. Two movies of electrochromic switches between neutral and oxidation states were provided in the Supporting Information. The amount of Q were calculated by integration of the current density and time obtained from Figure 4c as 0.922 mC/cm^2 and 0.918 mC/cm^2 for oxidation and reduction process at the first oxidation stage, respectively. The ratio of the charge density was 99.6%, indicating that charge injection/extraction was highly reversible during the electrochemical reactions. As shown in Figure 5, the electrochromic stability of the polyamide **Ib** film was determined by measuring the optical change as a function of the number of switching cycles. The electrochromic CE ($\eta = \delta OD/Q$) and injected charge (electroactivity) after various switching steps were monitored and summarized in Table 2 and 3. The electrochromic film of **Ib** was found to exhibit high CE up to 388 cm^2/C at 433 nm (320 cm^2/C at 1080 nm), and to retain more than 99% of their electroactivity after switching 10 000 times between 0 and 0.70 V (Figure 5A). As the applied switching potential increased to 1.10 V, a higher CE (433 cm^2/C at 835 nm) could be obtained and showed only 0.2% decay of its electroactivity after 3000 cycles (Figure 5B). Additional, Figure 6 show the long-term stability measured by keeping 5 h for each coloring

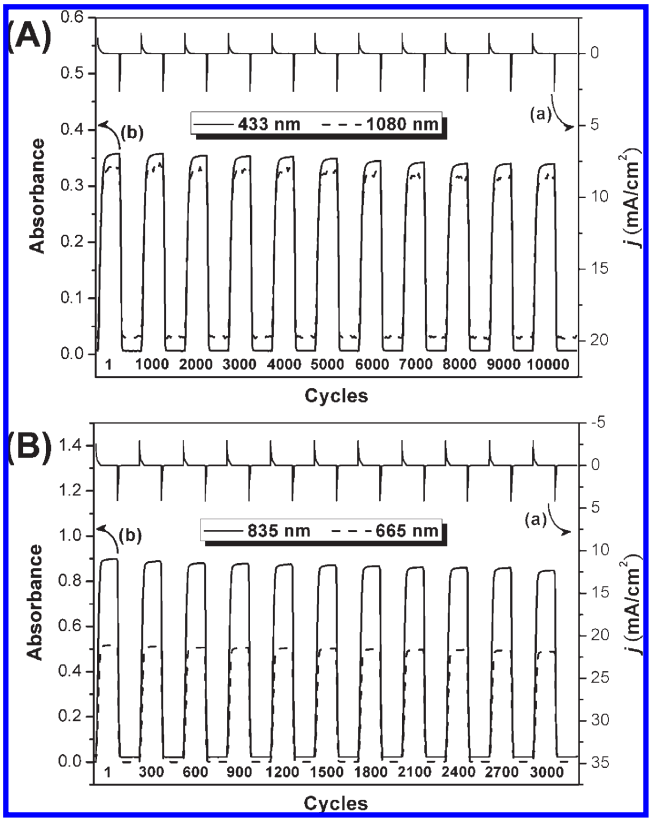

Figure 5. Electrochromic switching between (A) 0 and 0.70 V and (B) 0 and 1.10 V (vs Ag/AgCl) of polyamide **Ib** thin film (~65 nm in thickness) on the ITO-coated glass substrate (coated area: 1.1 cm × 0.5 cm) in 0.1 M TBAP/CH_3CN with a cycle time of 20 s. (a) Current consumption and (b) absorbance change monitored at the given wavelength.

Table 2. Optical and Electrochemical Data Collected for Coloration Efficiency Measurements of Polyamide Ib

cycling times[a]	δOD_{433}[b]	Q (mC/cm^2)[c]	η (cm^2/C)[d]	decay (%)[e]
1	0.358	0.922	388	0
1000	0.358	0.922	388	0
2000	0.355	0.923	384	1.03
3000	0.354	0.924	383	1.29
4000	0.352	0.925	381	1.80
5000	0.349	0.923	378	2.58
6000	0.344	0.920	374	3.61
7000	0.342	0.917	373	3.87
8000	0.340	0.918	370	4.64
9000	0.340	0.919	370	4.64
10000	0.339	0.918	369	4.89

[a] Switching between 0 and 0.70 (V vs Ag/AgCl). [b] Optical density change at 433 nm. [c] Ejected charge, determined from the in situ experiments. [d] Coloration efficiency is derived from the equation $\eta = \delta OD_{433}/Q$. [e] Decay of coloration efficiency after cyclic scans.

process at applied potentials of 0.70 and 1.10 V, respectively, and the highly stable electrochromic behaviors were observed, which reinforces and affords positive proof of these NIR electroactive aromatic polyamides with the potential for commercial applications. Considering the retained contrast ratio and electroactive stability during electrochromic operation, these novel polyamides show the highest electrochromic stability to the best of our knowledge comparing with other electrochromic polymers.[4]

Table 3. Optical and Electrochemical Data Collected for Coloration Efficiency Measurements of Polyamide Ib

cycling times[a]	δOD_{835}[b]	Q (mC/cm^2)[c]	η (cm^2/C)[d]	decay (%)[e]
1	0.876	1.889	464	0
300	0.867	1.889	459	1.08
600	0.859	1.890	455	1.94
900	0.856	1.891	453	2.37
1200	0.853	1.892	451	2.80
1500	0.850	1.890	450	3.02
1800	0.846	1.887	449	3.23
2100	0.840	1.884	446	3.87
2400	0.839	1.885	445	4.09
2700	0.837	1.887	444	4.31
3000	0.826	1.885	438	5.60

[a] Switching between 0 and 1.10 (V vs Ag/AgCl). [b] Optical density change at 835 nm. [c] Ejected charge, determined from the in situ experiments. [d] Coloration efficiency is derived from the equation $\eta = \delta OD_{835}/Q$. [e] Decay of coloration efficiency after cyclic scans.

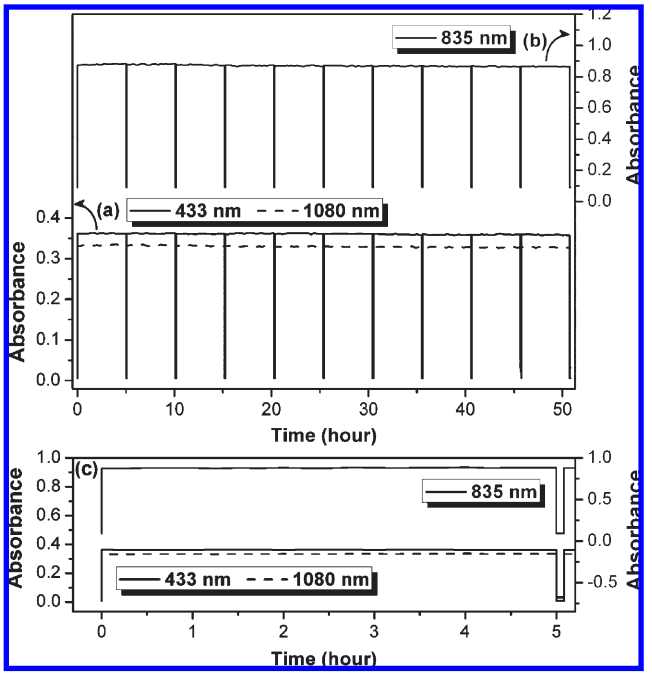

Figure 6. Potential step absorptometry during the continuous cycling test by switching potentials between (a) 0 and 0.70 V, (b) 0 and 1.10 V (vs Ag/AgCl), and (c) absorptometry for 1 switching cycle of polyamide **Ib** thin film (~65 nm in thickness) on the ITO-coated glass substrate (coated area: 0.9 cm × 0.6 cm) in 0.1 M TBAP/CH_3CN with a cycle time of 5 h and 5 min for coloring and bleaching processes, respectively.

Conclusions

A series of novel NIR electroactive TPPA-based aromatic polyamides were readily prepared from the newly synthesized diamine monomer, *N*,*N*′-bis(4-methoxylphenyl)-*N*,*N*′-di(4-methoxylphenyl)-1,4-phenylenediamine, with various aromatic dicarboxylic acids via the phosphorylation polyamidation reaction. Introduction of highly electron-donating (OMe_2)TPPA group to the polymer main chain not only stabilizes its cationic radicals and dications but also leads to good solubility and film-forming properties of the polyamides. In addition to high T_g and good thermal stability, all the obtained polymers reveal valuable electrochromic characteristics such as high contrast in, low switching times, high coloration efficiency, and excellent electrochromic/electroactive

reversibility. Thus, these characteristics suggest that these novel TPPA-based electrochromic aromatic polyamides have great potential for applications in both visible and NIR region.

Experimental Section

Materials. *N*,*N*′-Bis(4-aminophenyl)-*N*,*N*′-diphenyl-1,4-phenylenediamine[11] (TPPA-diamine; **2**′), *N*,*N*′-di(4-nitrophenyl)-1,4-phenylenediamine,[13] and 4-methoxy-4'-nitrodiphenylamine[14] were synthesized according to a previously reported procedure. Commercially available dicarboxylic acids such as trans-1,4-cyclohexanedicarboxylic acid (**3a**), 4,4′-oxidibenzoic acid (**3b**), and 2,2′-bis(4-carboxyphenyl)hexafluoropropane (**3c**) were purchased from Tokyo Chemical Industry (TCI) Co. and used as received. Commercially obtained anhydrous calcium chloride ($CaCl_2$) was dried under a vacuum at 180 °C for 8 h. TBAP (Acros) was recrystallized twice by ethyl acetate under nitrogen atmosphere and then dried in vacuo prior to use. All other reagents were used as received from commercial sources.

N,N′-Bis(4-nitrophenyl)-N,N′-di(4-methoxylphenyl)-1,4-phenylenediamine (***1***). Method A. To a solution of 10.18 g (29.06 mmol) of *N*,*N*′-di(4-nitrophenyl)-1,4-phenylenediamine, 15.28 g (64.00 mmol) of 4-iodoanisole, 10.28 g (74.37 mmol) of powdered anhydrous potassium carbonate, 4.65 g (73.22 mmol) of copper powder, and 2.00 g (7.56 mmol) of 18-crown-6-ether was stirred in 30 mL of *o*-dichlorobenzene under nitrogen atmosphere. After being heated at 180 °C for 24 h, the solution was filtered and cooled to precipitate red crystals. The precipitated red crystals were collected by filtration and purified by DMF/methanol. The product was filtered to afford 9.60 g (59% in yield) of red crystals.

Method B. To a solution of 2.60 g (7.90 mmol) of 1,4-diiodobenzene, 4.25 g (17.40 mmol) of 4-methoxy-4′-nitrodiphenylamine, 2.61 g (18.88 mmol) of powdered anhydrous potassium carbonate, 1.21 g (19.06 mmol) of copper powder and 0.50 g (1.89 mmol) of 18-crown-6-ether was stirred in 15 mL of *o*-dichlorobenzene under nitrogen atmosphere. After being heated at 180 °C for 24 h, the solution was filtered and cooled to precipitate red crystals. The precipitated red crystals were collected by filtration and purified by DMF/methanol. The product was filtered to afford 3.08 g (69% in yield) of red crystals. Mp: 224−227 °C (by DSC at a scan rate of 10 °C/min). FT-IR (KBr): 1584, 1308 cm^{-1} (NO_2 stretch). ^{1}H NMR (300 MHz, DMSO-d_6, δ, ppm): 3.76 (s, 6H, -OCH_3), 6.77 (d, J = 8.7 Hz, 4H), 7.03 (d, J = 8.7 Hz, 4H), 7.23 (d, J = 8.7 Hz, 4H), 7.28 (s, 4H), 8.03 (d, J = 8.7 Hz, 4H). ^{13}C NMR (75 MHz, DMSO-d_6, δ, ppm): 55.3, 115.1, 115.5, 125.0, 127.0, 128.4, 136.5, 137.9, 141.5, 152.7, 157.0. ESI-MS: calcd for $(C_{32}H_{26}N_4O_6)^+$, m/z 562.6; found, m/z 562.2.

N,N′-Bis(4-aminophenyl)-N,N′-di(4-methoxylphenyl)-1,4-phenylenediamine (***2***). In a 100 mL three-neck round-bottomed flask equipped with a stirring bar under nitrogen atmosphere, 1.16 g (2.06 mmol) of dinitro compound **1** and 0.05 g of 10% Pd/C were dispersed in 5 mL of ethanol and 30 mL THF. The suspension solution was heated to reflux, and 1 mL of hydrazine monohydrate was added slowly to the mixture. After a further 20 h of reflux, the solution was filtered to remove Pd/C, and the filtrate was cooled under nitrogen atmosphere. The precipitated product was collected by filtration and dried in vacuo at 80 °C to give 0.93 g (90% in yield) of pale yellow crystals with a mp of 194−197 °C (by DSC). FT-IR (KBr): 3444, 3359 cm^{-1} (N−H stretch). ^{1}H NMR (300 MHz, DMSO-d_6, δ, ppm): 3.68 (s, 6H, -OCH_3), 4.93 (s, 4H, -NH_2), 6.52 (d, J = 8.4 Hz, 4H), 6.67 (s, 4H), 6.75 (d, J = 8.4 Hz, 4H), 6.80 (d, J = 8.4 Hz, 4H), 6.86 (d, J = 8.7 Hz, 4H). ^{13}C NMR (75 MHz, DMSO-d_6, δ, ppm): 55.1, 114.0, 114.3, 121.1, 123.2, 126.1, 135.7, 140.9, 141.3, 144.4, 153.3. Anal. Calcd (%) for $C_{32}H_{30}N_4O_2$ (502.61): C, 76.47; H, 6.02; N, 11.15. Found: C, 76.24; H, 5.84; N, 11.02. ESI-MS: calcd for $(C_{32}H_{30}N_4O_2)^+$, m/z 502.6; found, m/z 502.4.

Polymer Synthesis. The synthesis of polyamide **Ib** was used as an example to illustrate the general synthetic route used to produce the polyamides. A mixture of 282.5 mg (0.56 mmol) of the diamine monomer **2**, 145.1 mg (0.56 mmol) of 4,4′-oxidibenzoic acid (**3b**), 60 mg of calcium chloride, 0.45 mL of triphenyl phosphite, 0.28 mL of pyridine, and 0.45 mL of NMP was heated with stirring at 105 °C for 3 h. The obtained polymer solution was poured slowly into 300 mL of stirred methanol giving rise to a stringy, fiberlike precipitate that was collected by filtration, washed thoroughly with hot water and methanol, and dried under a vacuum at 100 °C. Reprecipitations of the polymer by *N*,*N*-dimethylacetamide (DMAc)/methanol were carried out twice for further purification. The inherent viscosity and weight-average molecular weights (M_w) of the obtained polyamide **Ib** was 0.51 dL/g (measured at a concentration of 0.5 g/dL in DMAc at 30 °C) and 147 600 Da, respectively. The FT-IR spectrum of **Ib** (film) exhibited characteristic amide absorption bands at 3311 cm^{-1} (N−H stretch), 3037 cm^{-1} (aromatic C−H stretch), 2930, 2835 cm^{-1} (CH_3 C−H stretch), 1650 cm^{-1} (amide carbonyl), 1240 cm^{-1} (asymmetric stretch C−O−C), 1034 cm^{-1} (symmetric stretch C−O−C). Anal. Calcd (%) for $(C_{46}H_{36}N_4O_5)_n$ $(724.80)_n$: C, 76.23; H, 5.01; N, 7.73%. Found: C, 74.00; H, 5.06; N, 6.97%. The other polyamides were prepared by an analogous procedure.

Preparation of the Polyamide Films. A solution of polymer was made by dissolving about 0.4 g of the polyamide sample in 9 mL of DMAc. The homogeneous solution was poured into a 9 cm glass Petri dish, which was placed in a 90 °C oven for 5 h to remove most of the solvent; then the semidried film was further dried in vacuo at 160 °C for 8 h. The obtained films were about 20−35 μm in thickness and were used for solubility tests and thermal analyses.

Measurements. Fourier transform infrared (FT-IR) spectra were recorded on a PerkinElmer Spectrum 100 Model FT-IR spectrometer. Elemental analyses were run in a Heraeus Vario-EL-III CHNS elemental analyzer. ^{1}H NMR spectra were measured on a Bruker AC-300 MHz spectrometer in DMSO-d_6, using tetramethylsilane as an internal reference, and peak multiplicity was reported as follows: s, singlet; d, doublet. The inherent viscosities were determined at 0.5 g/dL concentration using Tamson TV-2000 viscometer at 30 °C. Gel permeation chromatographic (GPC) analysis was performed on a Lab Alliance RI2000 instrument (one column, MIXED-D from Polymer Laboratories) connected with one refractive index detector from Schambeck SFD Gmbh. All GPC analyses were performed using a polymer/DMF solution at a flow rate of 1 mL/min at 70 °C and calibrated with polystyrene standards. Thermogravimetric analysis (TGA) was conducted with a PerkinElmer Pyris 1 TGA. Experiments were carried out on approximately 6−8 mg film samples heated in flowing nitrogen or air (flow rate = 20 cm^3/min) at a heating rate of 20 °C/min. DSC analyses were performed on a PerkinElmer Pyris 1 DSC at a scan rate of 10 °C/min in flowing nitrogen (20 cm^3/min). Electrochemistry was performed with a CH Instruments 611B

(13) Rozalska, I.; Kulyk, P.; Kulszewicz-Bajer, I. *New J. Chem.* **2004**, *28*, 1235.
(14) Liou, G. S.; Lin, H. Y. *Macromolecules* **2009**, *42*, 125.

electrochemical analyzer. Voltammograms are presented with the positive potential pointing to the left and with increasing anodic currents pointing downward. Cyclic voltammetry (CV) was conducted with the use of a three-electrode cell in which ITO (polymer films area about 0.5 cm × 1.1 cm) was used as a working electrode. A platinum wire was used as an auxiliary electrode. All cell potentials were taken by using a homemade Ag/AgCl, KCl (sat.) reference electrode. Spectroelectrochemical experiments were carried out in a cell built from a 1 cm commercial UV−visible cuvette using Hewlett-Packard 8453 UV−visible diode array and Hitachi U-4100 UV−vis−NIR spectrophotometer. The ITO-coated glass slide was used as the working electrode, a platinum wire as the counter electrode, and a Ag/AgCl cell as the reference electrode. CE (η) determines the amount of optical density change (δOD) at a specific absorption wavelength induced as a function of the injected/ejected charge (Q; also termed as electroactivity) which is determined from the in situ experiments. CE is given by the equation: $\eta = \delta\mathrm{OD}/Q = \log[T_b/T_c]/Q$, where η (cm^2/C) is the coloration efficiency at a given wavelength, and T_b and T_c are the bleached and colored transmittance values, respectively. The thickness of the polyamide thin films was measured by alpha-step profilometer (Kosaka Lab., Surfcorder ET3000, Japan). Colorimetry measurements were obtained using a Minolta CS-100A Chroma Meter. The color coordinates are expressed in the CIE 1931 Yxy color spaces.

Supporting Information Available: Two movies of electrochromic switches between neutral and oxidation states (AVI). Additional tables of inherent viscosity, molecular weights, solubility behavior, and thermal properties; additional figures of IR of monomers and polyamide, TGA and DSC traces of polyamides (PDF). This material is available free of charge via the Internet at http://pubs.acs.org.